Available online at www.sciencedirect.com
ScienceDirect
Journal of Power Sources 172 (2007) 476–480
JOURNAL OF POWER SOURCES
www.elsevier.com/locate/jpowsour

Short communication

Electrochemical properties of ultra-long, aligned, carbon nanotube array electrode in organic electrolyte

Hao Zhang *, Gaoping Cao, Yusheng Yang

Research Institute of Chemical Defense, West Building, No. 35 Huayuanbei Road, Beijing 100083, China

Received 28 April 2007; received in revised form 11 July 2007; accepted 18 July 2007
Available online 6 August 2007

Abstract

The electrochemical properties of an electrochemical double-layer capacitor electrode based on an ultra-long (500 μm), aligned, carbon nanotube array (ACNTA) in Et_4NPF_6/propylene carbonate electrolyte are examined. The specific capacitance of the ACNTA electrode in an organic electrolyte is 24.5 F g^{-1}, which is larger than that obtained in an aqueous electrolyte. The results of ac impedance measurements show that the ACNTA electrode gives a high power density and an excellent rate capability in an organic electrolyte. It is shown that the ACNTA electrode has a lower equivalent series resistance and a better rate capability than activated carbon electrode. This is due to the fact that ACNTA possesses a larger pore size and a more a regular pore structure. Both these features are conformed by scanning electron microscopic and nitrogen gas adsorption studies.

Keywords: Aligned carbon nanotube array; Electrochemical double-layer capacitor; Electrochemical properties; Ion diffusion resistance; Organic electrolyte; Specific capacitance

1. Introduction

Electrochemical double-layer capacitors (EDLCs) are power sources that store energy within the electrochemical double-layer formed at a solid/solution interface [1–5]. The devices have attracted great interest because of their possible usage in power sources for electric vehicles that would have much higher power density and longer cycle life than batteries [1]. Activated carbons (ACs) are the electrode materials that are used most frequently in EDLCs, but have several intrinsic disadvantages [1,2], such as low conductivity and irregular pore structures that result in limited energy and power densities. Thus, the most effective way to improve EDLC performance is to develop new electrode materials with high conductivity and regular pore structures, such as properly designed carbon aerogels [3], nanoporous carbons [5], and aligned carbon nanotube arrays (ACNTA).

Due to their nanometer size and outstanding properties, carbon nanotubes (CNTs) are of great interest for many applications, namely: batteries [6], storage of hydrogen [7], flat panel displays [8,9], chemical sensors [10], and EDLCs [11]. Several researchers [12–15] have explored CNT-based EDLC electrodes, in which, most of the CNTs have possessed entangled structures. Thus, the CNT electrodes have had irregular pore structures that would not facilitate the fast transfer of electrolyte ions and there by limit any improvement in the electrochemical performance of EDLCs. Compared with entangled CNT (ECNT), ACNTAs have more regular pore structures and conductive paths, and therefore higher effective specific surface areas (SSAs) [16] and lower ion diffusion resistances. An ACNTA can be grown directly or pasted on a current-collector to obtain an EDLC electrode [17]. Although the direct growth of ACNTA on a bulk metal [18,19] is attractive, the parameter space and growth window are narrow [20]. Given that the growth of ACNTAs on silica substrates is a mature process, a cut-paste method was adopted in a previous investigation [17]. The resulting ACNTA electrode had excellent rate capability in aqueous electrolyte. Compared with an aqueous electrolyte, use of an organic electrolyte enabled an EDLC to sustain higher voltage and have higher specific energy. In this study, we examine the electrochemical properties of a 500-μm ACNTA electrode in an organic electrolyte by means of a galvanostatic charge/discharge method and ac impedance spectroscopy. The results show that ACNTA electrode has a specific capacitance of 24.5 F g^{-1} and an excellent rate capability in organic electrolyte.

* Corresponding author. Tel.: +86 10 66705840; fax: +86 10 66705840.
E-mail address: etwas-chang@sohu.com (H. Zhang).

0378-7753/$ – see front matter © 2007 Elsevier B.V. All rights reserved.
doi:10.1016/j.jpowsour.2007.07.060

2. Experimental

2.1. ACNTA growth

A ferrocene–xylene chemical vapour deposition (CVD) system was used for the growth of a vertically aligned CNT array on a silica substrate [17]. The growth was carried out in a horizontal quartz tube that was housed in a muffle furnace. The optimium conditions for the process are as follows. Ferrocene was dissolved in xylene (0.01 g ml^{-1}). The substrate was gradually heated to 800 °C in flowing argon. The latter was replaced with a carrier gas mixture (300 sccm Ar + 50 sccm H_2) and injection of the ferrocene–xylene solution was commenced. The prepared solution was injected into the quartz tube through a capillary using a syringe pump (feed speed 0.10 mL min^{-1}) and the aligned CNTs began to grow on the silica substrate. A 500-μm CNT array was obtained by setting the growth time at 2 h.

2.2. ACNTA electrode preparation

A 500-μm ACNTA, with 6 mm × 4 mm apparent area, was removed from the silica substrate with a razor blade. A layer of graphite milk (DAG-2, Qingdao Xiyou Fine Graphite Chemicals Industry Co. Ltd., 50 μm in thickness) was cast on to a 4.0 cm × 0.8 cm nickel foil and then the ACNTA was pasted immediately on the nickel foil to prepare an electrode [17]. After pasting, the film was dried in an oven at 120 °C for 1 h. To provide a material for comparative studies, an activated carbon (prepared from ground apricot stone, activated by sodium hydroxide at 700 °C for 1 h) was used to fabricate EDLC electrodes. The activated carbon powder was mixed and kneaded with 3 wt.% PTFE and 5 wt.% acetylene black and then pasted on a nickel foil current-collector with the assistance of graphite milk.

2.3. ACNTA electrode characterization

The SSA and pore-size distribution (PSD) of the respective electrode materials were obtained from analysis of the desorption branch of N_2 gas isotherms (taken with a Micrometrics ASAP 2010 instrument at 77 K) using the density function theory (DFT) method. Scanning electron microscopy (SEM) and transmission electron microscopy (TEM) were used to characterize the microstructures of the ACNTA electrodes. The electrochemical properties of ACNTA and AC electrodes were examined in three-electrode systems, with platinum and AC electrodes as reference and counter electrodes, respectively. The electrolyte solution was 1 M Et_4NPF_6 in propylene carbonate. Measurement of specific capacitance was performed by means of galvanostatic charge/discharge cycling using a BT2000

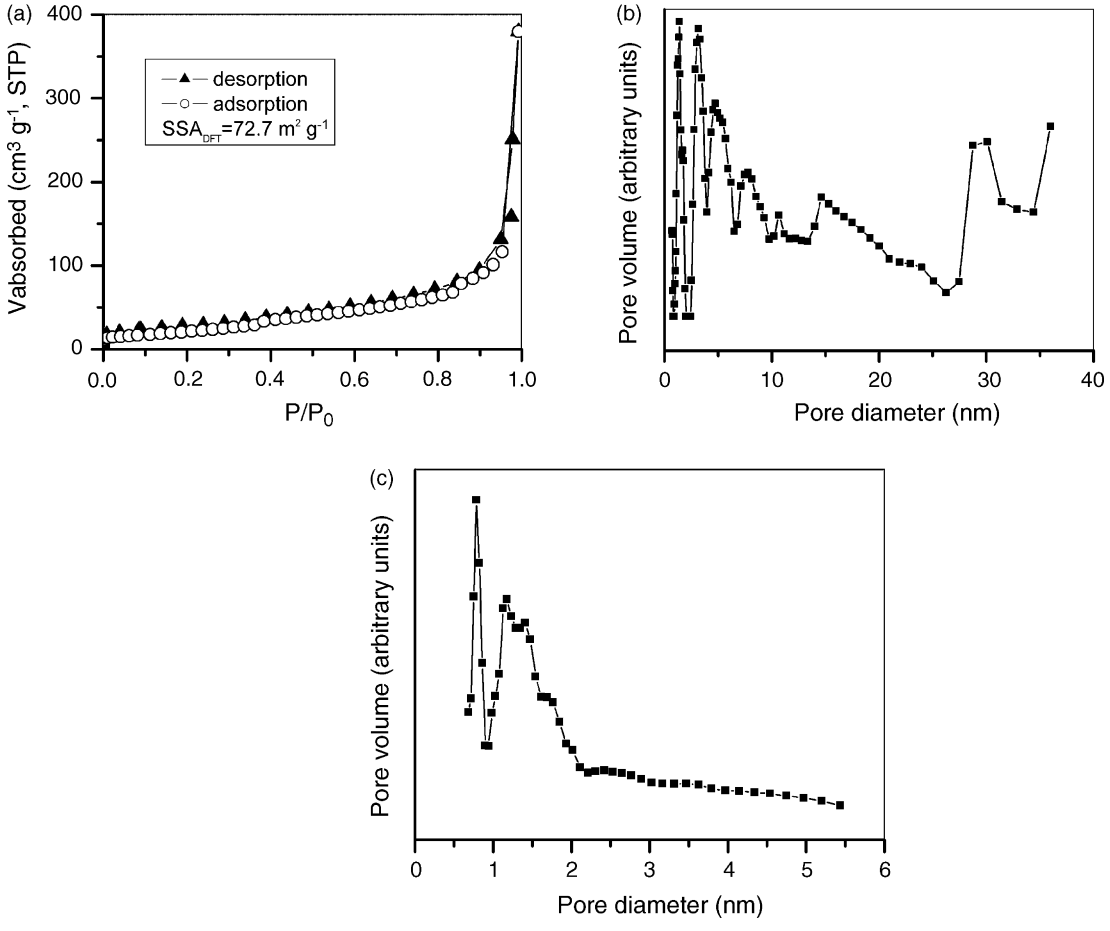

Fig. 1. (a) Nitrogen absorption/desorption isotherms of ACNTA. DFT pore-size distribution of (b) ACNTA and (c) AC.

(Arbin instruments) test station. The ac impedance studies were conducted with a Solartron 1280Z electrochemical test station, which applied an alternating current in the frequency range from 20 kHz to 0.001 Hz, with a 5 mV amplitude, on the dc voltage of −1 V versus platinum.

3. Results and discussion

Fig. 1a shows N_2 adsorption/desorption isotherms of the as-synthesized ACNTA. The shape of the isotherms exhibits the features of type-II adsorption/desorption isotherms according to the International Union of Pure and Applied Chemistry (IUPAC) classification, which agrees with some other reported results [16,21]. The SSA of ACNTA, calculated using the DFT method, is 72.7 $m^2\ g^{-1}$. From the PSD plots of ACNTA (Fig. 1b) and AC (Fig. 1c), it is seen that the pore diameters of ACNTA are mainly distributed over the mesopore range (2–50 nm) and are much larger than those of the AC (<2 nm).

A scanning electron micrograph of the 500 μm aligned CNT array is presented in Fig. 2a. A close examination at the side of the array (Fig. 2b) reveals that the nanotubes are densely packed and well aligned. The TEM image of an individual CNT (the inset in Fig. 2b) indicates that the CNT is clean and free from amorphous carbon. The outer and inner diameters of the CNT are 14 and 3 nm, respectively. Therefore, the wall number of the CNT is $(14-3)/0.34+1 \approx 33$ [22]. If the mean wall number of CNT in the ACNTA is 33, the theoretical specific surface area of the CNT is $2630/33 \approx 80\ m^2\ g^{-1}$, which is consistent with the value obtained by the N_2 adsorption method (72.7 $m^2\ g^{-1}$). The relationship between the wall numbers of CNT and the SSA of ACNTA implies that the SSA, and thereby the specific capacitance, of the ACNTA electrode can be increased by decreasing the wall numbers of CNT. Detailed studies into factors such as controlling the wall numbers and length of ACNTA, and the effects of these on electrode performance are being carried out and will be discussed in a later communication. Fig. 2c is a SEM image of the CNT in the ACNTA electrode. It is seen that the nanotubes are still densely packed and the individual CNTs are still quite straight. This suggests that the cut-paste method does not damage the microstructure of the ACNTA. The inset in Fig. 2c is an optical image of a 0.5 mm ACNTA on a nickel foil current-collector, a coin of 1.4 mm in thickness and 22.0 mm in diameter is included to serve as a size reference. The ACNTA electrode is thicker than normal AC-based EDLC electrodes (0.1–0.3 mm

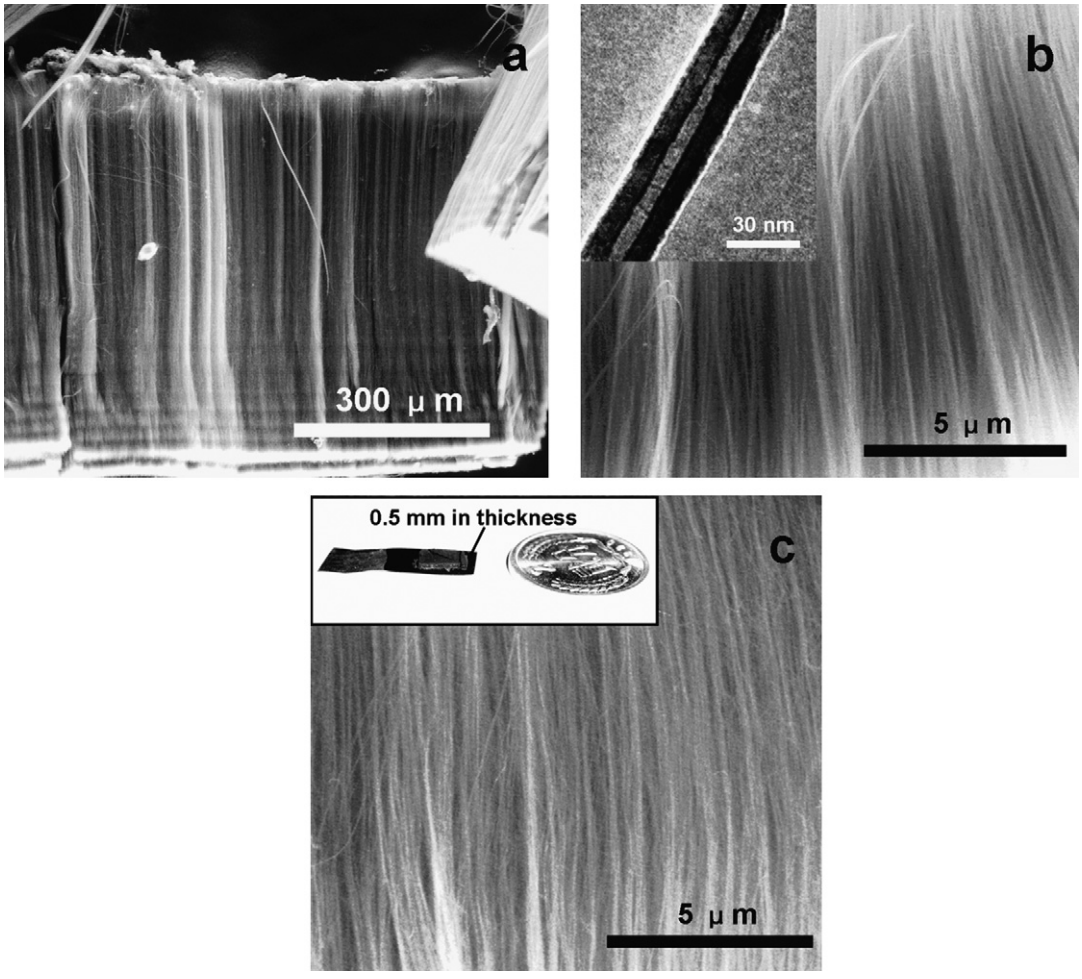

Fig. 2. (a) Scanning electron micrographs of: (a) 500-μm ACNTA; (b) CNT in the array, inset is the TEM image of an individual CNT in the array; (c) CNT in the ACNTA electrode, inset is a picture of a 0.5 mm ACNTA on a nickel foil current-collector. A coin of 1.4 mm in thickness and 22.0 mm in diameter is given as a size reference.

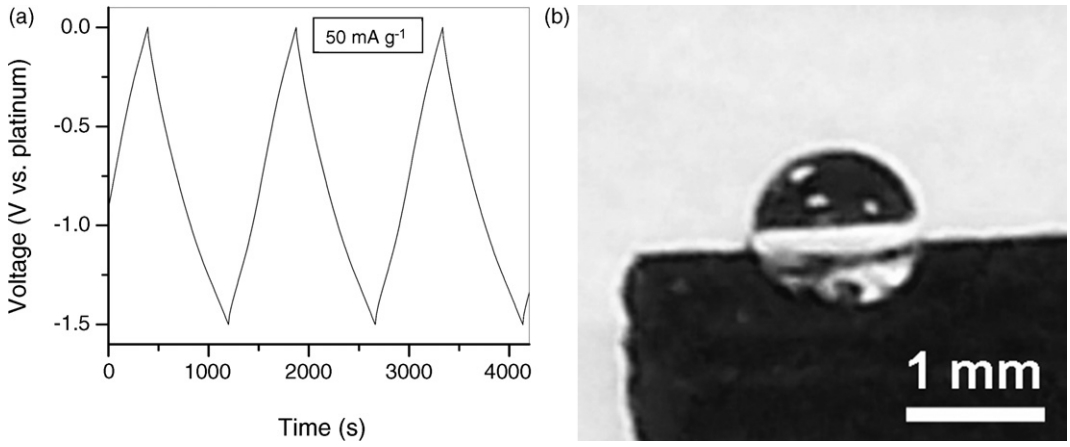

Fig. 3. (a) Charge–discharge cycles at a constant current density of 50 mA g^{-1}. (b) A water droplet on CNT surface.

in thickness) and this indicates that our research is close to practical application. Thick electrodes are advantageous to increase energy density, in such cells the active material can occupy high ratios in terms of both volume and weight.

The specific capacitance of the ACNTA in an organic electrolyte, calculated from the discharge slope (Fig. 3a) measured at a current density of 50 mA g^{-1}, is 24.5 F g^{-1}, which is larger than the specific capacitance of ACNTA (14.1 F g^{-1}) in an aqueous electrolyte [17]. This phenomenon has never been reported for AC-based EDLCs. Fig. 3b is a photograph of a water droplet on the CNT surface; the high contact angle (>140°) indicates the hydrophobic property of CNT. Therefore, aqueous electrolyte cannot soak the ACNTA electrode thoroughly, which results in a decrease in the double-layer surface area, and thus the specific capacitance. The hydrophilic property of CNT should be improved, which can be realized by surface treatment [23], to make ACNTA electrode obtain higher specific capacitance in aqueous electrolyte.

Fig. 4a gives Nyquist plots of ACNTA (20 kHz to 0.01 Hz) and AC electrodes (20 kHz to 0.001 Hz) with the same apparent area and thickness (6 mm × 4 mm × 0.5 mm). Both plots show typical EDLC characteristics. Compared with the AC electrode, the ACNTA electrode has a lower equivalent series resistance (ESR, 47.4 Ω) and a much higher characteristic frequency [24] (f_0, 0.1 Hz). These features are indicative of higher power density and better rate capability. Ion diffusivity plays a key factor in the realization of EDLCs with high power density and excellent rate capability. The AC electrode has a high ion diffusion barrier in the inner region of the electrode (Fig. 4b) because of its small pore size (Fig. 1c) and irregular pore structure.

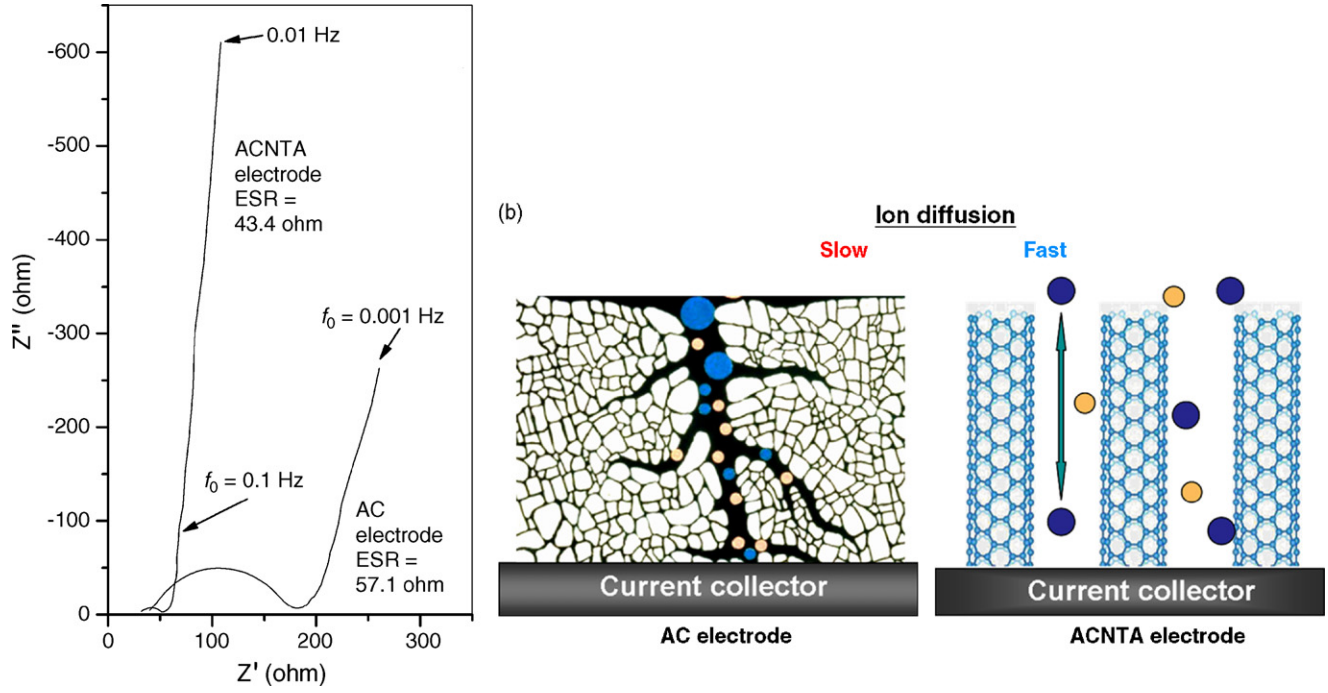

Fig. 4. (a) Nyquist plots of ACNTA (20 kHz–0.01 Hz) and AC (20 kHz–0.001 Hz) electrodes. (b) Schematic models of ion diffusivity in AC and the ACNTA electrodes.

This factor results in high internal resistance and inferior power performance. Compared with AC, the ACNTA electrode has a regular pore structure (Fig. 2c) and large pore size (Fig. 1b), which result in superior ion diffusivity, higher power density, and better rate capability. Given that the conductivity of CNT is excellent and each CNT is contacted directly to the current-collector, the ESR of the ACNTA electrode is dominated by the contact resistance between the bottom of the ACNTA and the top of the current collector. By improving the paste technique or growing ACNTA directly on current collectors, the equivalent series resistance (ESR) of the ACNTA electrode can be lowered so that the ACNTA electrode can achieve better rate capability and higher power density.

4. Conclusion

An ACNTA electrode has been prepared to retain the regular pore structure and large pore size of the original CNT array. This mesoporous ACNTA electrode exhibits a specific capacitance of $24.5\,F\,g^{-1}$ in an organic electrolyte. The value is larger than that measured in aqueous electrolyte and is due to the fact that the aqueous electrolyte cannot soak the hydrophobic ACNTA electrode thoroughly. The specific capacitance of ACNTA is lower than that of AC because the specific surface area of nanotubes is too low and it is difficult to enhance significantly the surface area of nanotubes. Further improvements in the capacitance of the ACNTA electrode are expected through fabricating conducting polymer/ACNTA or metal oxide/ACNTA composite electrodes. The ACNTA electrode has a lower ESR and a much better rate capability than the AC electrode. This is because the ACNTA possesses a larger pore size and a more regular pore structure, as revealed by SEM and nitrogen gas adsorption studies. Further improvements in performance may be achieved by improving the paste technique or growing ACNTA directly on current-collectors, such as Al and Cu foils.

Acknowledgments

Financial support from the National Science Foundation of China (No. 20633040) is gratefully acknowledged. We thank Prof. Zhennan Gu (Peking University) for his valuable help.

References

[1] R. Kötz, M. Carlen, Electrochim. Acta 45 (2000) 2483.
[2] R. Signorelli, J. Schindall, J. Kassakian, Proceedings of the 14th International Seminar on Double Layer Capacitors and Similar Energy Storage Devices, FL, December 6–8, 2004, p. 49.
[3] B. Fang, L. Binder, J. Power Sources 163 (2006) 616.
[4] B.E. Conway, Electrochemical Supercapacitor, Kluwer-Academic/Plenum, New York, 1999, pp. 12–13.
[5] A. Jänes, E. Lust, Electrochem. Commun. 7 (2005) 510.
[6] J. Shu, H. Li, R. Yang, Y. Shi, X. Huang, Electrochem. Commun. 8 (2006) 51.
[7] A. Dillon, K. Jones, T. Bekkedahl, C. Kiang, D. Bethune, M. Heben, Nature 386 (1997) 377.
[8] J. Wildoer, L. Venema, A. Rinzler, R. Smalley, C. Dekker, Nature 391 (1998) 59.
[9] Z. Ren, Z. Huang, J. Xu, J. Wang, P. Bush, M. Siegal, P. Provencio, Science 282 (1998) 1105.
[10] J. Kong, N. Franklin, C. Zhou, M. Chapline, S. Peng, K. Cho, H. Dai, Science 287 (2000) 622.
[11] R. Baughman, A. Zakhidov, W. de Heer, Science 297 (2002) 787.
[12] C. Niu, E. Sichel, R. Hoch, D. Moy, H. Tennent, Appl. Phys. Lett. 70 (1997) 1480.
[13] C. Liu, A. Bard, F. Wudl, I. Weitz, J. Heath, Electrochem. Solid-State Lett. 2 (1999) 577.
[14] C. Emmenegger, P. Mauron, A. Zuttel, C. Nutzenadel, A. Schneuwly, R. Gallay, L. Schlapbach, Appl. Surf. Sci. 162/163 (2000) 452.
[15] C. Emmenegger, P. Mauron, P. Sudan, P. Wenger, V. Hermann, R. Gallay, A. Zuttel, J. Power Sources 124 (2003) 321.
[16] D. Zilli, P. Bonelli, A. Cukierman, Nanotechnology 17 (2006) 5136.
[17] H. Zhang, G. Cao, Y. Yang, Nanotechnology 18 (2007) 195607.
[18] T. Hiraoka, T. Yamada, K. Hata, D. Futaba, H. Kurachi, S. Uemura, M. Yumura, S. Iijima, J. Am. Chem. Soc. 128 (2006) 13338.
[19] S. Talapatra, S. Kar, S. Pal, R. Vajtai, L. Cl, P. Victor, M. Shaijumon, S. Kaur, O. Nalamasu, P. Ajayan, Nat. Nanotechnol. 1 (2006) 112.
[20] G. Zhang, D. Mann, L. Zhang, A. Javey, Y. Li, E. Yenimez, Q. Wang, J. McVittie, Y. Nishi, J. Gibbons, H. Dai, Proc. Natl. Acad. Sci. 102 (2005) 16141.
[21] Q. Yang, P. Hou, S. Bai, M. Wang, H. Cheng, Chem. Phys. Lett. 345 (2001) 18.
[22] H. Cheng, Carbon nanotubes—Synthesis, Microstructure, Properties and Applications, Chemical Engineering Press, Beijing, 2002, pp. 186–188.
[23] B. Yoon, S. Jeong, K. Lee, H. Kim, C. Park, J. Han, Chem. Phys. Lett. 388 (2004) 170.
[24] P. Taberna, P. Simon, J. Fauvarque, J. Electrochem. Soc. 150 (2003) A292.